Original article

The Ion Partition Detected in Homeopathically Manufactured Medicine Cuprum metallicum and Controls

Michel Van Wassenhoven[1*], Bernard Nysten[2], Martine Goyens [3], Pierre Dorfman [4], Philippe Devos [5], Delphine Magnin [2] .

1 - Coordinator of DynHom Research Project, Chastre, Belgium.
2 - Institute of Condensed Matter and Nanosciences (Bio and Soft Matter), Université catholique de Louvain, Louvain-la-Neuve, Belgium
3 - Pharmaceutical Association for Homeopathy, Wépion, Belgium.
4 - Madeleine et Rolland Conte Endowment Fund. Meyzieu, France.
5 - Unio Homoeopathica Belgica, Evergem, Belgium.

*michelvw@homeopathy.be – https://orcid.org/0000-0002-8047-7735

Abstract

Background: Homeopathy is highly controversial. The main reason for this is its use of very highly dilute medicines (high homeopathic potencies, HHP), diluted beyond the Avogadro/Loschmidt limit. Research using Nano Tracking Analysis has demonstrated the presence of particles in HHPs. This study aims to verify the results of a previous publication that identified the ionic composition of these particles in all dilutions. **Methods**: We used *Scanning Electron Microscopy* & Energy Dispersive X-Ray Spectroscopy (SEM-EDX) to examine dilutions of a commonly used homeopathic medicine, an insoluble metal, Cuprum metallicum, for the presence of particles (NPs). The homeopathic medicines tested were specially prepared according to the European pharmacopoeia standards. We compared the homeopathic dilutions/dynamizations of copper with simple dilutions and dynamized lactose controls. **Results**: We observed an ionic diversity common to all preparations including HHPs but also significant differences in the relative quantity of each ion between manufacturing lines of homeopathic copper and lactose controls. The probability that the observed differences could have occurred chance alone (especially above Avogadro limit) can be rejected at $p < 0.001$**.** The essential component of these homeopathic medicines is sodium hydrogen carbonate, modulated by some other elements and by its quantity, size and shape. **Conclusion**: Homeopathic medicines made of Cuprum metallicum do contain material with a specific ionic composition even in HHPs diluted beyond the Avogadro/Loschmidt limit. This specificity can be attributed to the manufacturing process. This material demonstrates that the step-by-step process (dynamized or not) does not match the theoretical expectations of a dilution process. The starting material and dilution/dynamization method influences the nature of these NPs. Further measurements are needed on other raw materials using the same controls (solvent and simply diluted manufacturing lines) to support these findings. The role of sodium bicarbonate must be carefully studied in the future.

Keywords: Nanoparticles; Particles; Cuprum metallicum, Copper; Lactose; Homeopathy; Potentization; Dynamization; Pharmacology; *Scanning Electron Microscopy* & Energy Dispersive X-Ray Spectroscopy (SEM-EDX); Sodium hydrogen carbonate; Sodium bicarbonate.

Introduction

Homeopathic practitioners daily prescribe homeopathic medicines and patients take these regularly. There is an increasing need for a clear explanation of the nature of these medicines. Recent studies

OPEN ACCESS

indicate that homeopathically-prepared medicines (HMs) contain nanoparticles (NPs) [1-9]. Previous publications [10-14] using NMR relaxation have revealed the involvement of nanobubbles and/or nanoparticles and/or nanometric superstructures in high potentizations.

A recent RCT-literature audit [15-16] once more confirmed the existence of a specific effect of homeopathic treatments. Despite this, skeptics continue to insist that HMs are mere placebos containing no active material in any form [17].

This debate about plausibility and evidence [18-22] can only be settled by fundamental research. Skeptics have focused on the dilution of bulk source material beyond Avogadro's number and have ignored the fact that the actual manufacturing process is more than simple dilution – it involves step-by-step potentization (for water-soluble materials), also called a "dilution-dynamization" process which is described in the European Pharmacopoeia [23]. The potentization process is performed using a certified machine which normally provides 100 calibrated vertical shocks at each dilution. The dilution process must be 1 part of the material for 9 parts of solvent (D or X potency) or 1 part of the material for 99 parts of solvent (C or Korsakov potency). The containers are always pharmaceutical soda-lime-silicate glass ISO-719, ISO4802-1, Ph-Eur 3.2.1.; USP <660>: =< 0.85 ml 0.02N HCL/g. A new container is used at each step in the manufacture of C and D potencies.

The purpose of the present exploratory study is to replicate and extend the characterization of colloidal particles in homeopathically-made Cuprum metallicum (copper source) [1] following good pharmaceutical practice (GPP). The samples come from a pool of 6 different production lines, up to 30C potency, which have already been characterized using Nano Tracking Analysis (NTA) [2]. We compare these samples with three controls: solvent, potentized lactose, and simply diluted copper.

Materials and Methods

Rationale: Anticipating a need to detect low concentrations of poly-dispersed particles of different sizes, shapes, surface properties, and compositions [1-4], we used Field Emission Gun *Scanning Electron Microscopy* & Energy Dispersive X-Ray Spectroscopy (FED-SEM and EDX) [24-26].

We chose copper as the initial source material for HMs because it has already been characterized [1-2], because of the well-known role of copper in the mitochondrial enzyme cytochrome c oxidase [27], and because there is an extensive homeopathic medicine literature, including a randomized controlled trial [28-41].

Homeopathically-manufactured medicines

The medicines and controls were made in our own laboratory located in Wepion (Belgium), under a validated (ISO 5) laminar flow ("Thermo Heragard Eco 1.2 horizontal" B75/180). Our pharmacist followed the European pharmacopeias which describe precisely how the manufacturing process must be carried out according to the homeopathic tradition. The triturations were performed manually following the standardized rules and controls of good pharmaceutical practice (GPP). We used monohydrated, moderately fine lactose (particle x 50 = 240 µm) ABC Chemicals. Aut.84GIR05797. Ph. Eur.+ monogr. Lot 19I04-B02-194990 Exp. 30-04-2022. Cond. 30-10-2019. The water used is deionized water drawn directly from the tap after having released some water first. The tip of the tap goes directly into a flask containing ethanol to avoid ambient contamination. Purifying apparatus is Millipore Milli-RX 45 serial number FSDM 96292D. 50 g of copper powder is provided by Remedy Bank: Sigma 203122 lot #MKBS 4830 Pcode 1001 89 73 74 containing 99.999% copper. The brown pharmaceutical 30 cc flasks which are used are soda-lime-silicate glass ISO-719,

ISO4802-1 closed by tight plastic drop-caps with an under-screwed polypropylene closure system PhEur 3.1.3 "Polyolefines"; PN*18*K*S1 0.6 of PPH.

The pharmacist's equipment included a mask (possible toxic effect on respiratory tract), protective glasses (possible irritating effect), shoe protections, a white apron, no perfume, a head cap, and gloves (during triturations). Hands were washed meticulously before carrying out any operation.

100 mg of copper was placed on a paper and 9900 mg of lactose was weighed for the trituration. According to the method PhEur 4.1.2., the vehicle was added carefully in small quantities whilst grinding until the entire vehicle was incorporated. The duration of trituration was one hour to obtain a 1C potentization. The intensity of trituration is sufficient to ensure homogeneity, with a particle size after trituration not exceeding 100 µm. The result is an ultra-fine, dry powder with a final mass between 9317 mg and 9638 mg (6 separate manufacturing lines were set up after the trituration processes); the weight loss is due to adhesion onto the pestle and mortar.
After washing and passivating the mortar, pestle, and spatula, the same process was carried out starting with 100 mg of the 1C and 9900 mg of lactose. Following the same procedure with 100 mg of 2C and 9900 mg of lactose, we then produced the 3C dilution. From this step onward the mixture becomes soluble in water. We decided to avoid the use of an alcohol-water mixture lest the alcohol alters the measurements; it might also add unwanted contaminants to the solution. All further steps were performed in washed and passivated 30cc new glass containers. 0.2 g of 3C was added to 19.8 g of water and dynamized (100 +/-2 shocks in 2 seconds using a Labotics© certified and validated dynamizer "Dynamat©") to obtain a 4C potency. Further dynamizations were produced by the same process, each time in a new container, adding 0.2 g of the previous dynamization in 19.8 g of water to produce 5C, 6C, etc. up to 30C.

The potentized lactose controls were produced in the same way, including the 3 first trituration steps but starting from 10 g of pure lactose to produce the 1C. The simply diluted copper control was prepared following the same successive steps after 3 triturations. Further dilutions were prepared in water but without the dynamization process. We also prepared one additional pure water control (simply pre-filtered using a 0.1 µm filter) and one lactose control simply diluted in pure water 1/100. Each flask was labeled with an abbreviated code indicating the raw material including the level of dilution or potentization, line number, and manufacturing date.

Lyophilization process

Freeze drying, also known as lyophilization or cryodesiccation, is a low-temperature dehydration process that involves freezing the product, lowering the pressure, then removing the ice by sublimation. This contrasts with most conventional methods of dehydration that evaporate water using heat. Because of the low temperature used in this process, the quality of the dehydrated product is excellent, and the original shape of the product is maintained.
We started with 6 manufacturing lines of each raw material including controls. Since we were able to demonstrate that the particles detected by NTA in each sample are similar for the same level of dilution and dynamization, for the same raw material, and the same manufacturing process, the separate samples from the 6 manufacturing lines were combined into a single 100 ml sample in a 500 cc borosilicate flask. Samples are frozen at -40°C. The initial step of the lyophilization process takes place at -90°C and 0.1 bar for about 22.5 hours. The residual 5 ml sample is transferred to a 10 cc borosilicate flask, frozen again, and lyophilized for a further 13 h. Flasks are weighed empty and at the end of the process, allowing the harvested material to be weighed. We used a lyophilizator CHRIST Alpha 2-4 LSC basic.

Randomization and blinding

A full double-blind procedure is implemented. Borosilicate flasks are randomly numbered before the lyophilization process. After weighing, the bottle is tightly closed with a glass stopper. Samples are randomly distributed in racks and analyzed by SEM-EDX measurements. The measurement reports arrive back identified only by the random number. These are then decoded and reclassified according to production line and dilution.

***Scanning Electron Microscopy* & Energy Dispersive X-Ray Spectroscopy (SEM-EDX)** [24].

The first step of a scientific evaluation is to thoroughly observe the form of the material. For this purpose, we have a magnifying glass or an optical microscope. However, using light precludes seeing anything smaller than the wavelength of light which makes observing any nanostructure extremely difficult. The Scanning Electron Microscope (SEM) used for this study utilizes an electron beam whose wavelength is much shorter than that of light and which can therefore resolve structures down to the nanometer scale. (1 nm = billionth of a meter = 10^{-9}m.)
The Scanning Electron Microscope gives a clear view of the surface morphology at the nanometre scale, which is not possible with an Optical Microscope (OM). Moreover, as it can provide images with greater focal depth, enlargement of the rough surface structure of the specimen provides 3-dimensional images, giving a similar sense as when we look at a substance with the naked eye.

SEM utilizes electrons to show an enlarged image of a specimen. Since an electron beam has a shorter wavelength than light, it enables us to observe smaller objects than can be seen with the OM. The term "resolution" refers to the smallest separation between two objects which can be observed as distinct objects. The resolution of the human eye is said to be 0.2 mm, whilst the SEM's resolution is 1 to 4 nm. SEM forms the image using the secondary electrons generated from the surface of the specimen.

From the spot illuminated by the electron beam, various signals, such as secondary electrons, backscattered electrons, characteristic X-rays, and cathodoluminescence, are emitted depending on the form of the specimen, and the density of the substance, and the elements comprising it.
Scanning Electron Microscope (SEM) normally detects secondary electrons to form an image for viewing. As the intensity of the secondary electrons generated varies according to the angle of the incident electrons onto the specimen surface, subtle variations in the roughness of the surface can be detected by the signal intensity. Moreover, SEM allows us to visualize the surface of the sample since SEM creates an image by detecting reflected electrons.

Energy Dispersive X-Ray Spectroscopy (EDX or EDS) provides a spectrum of the energy density of emitted X-rays using a combination of the Li-doped Si semiconductor detector and the Multi-Channel Analyzer (spectrum analyzer). All elements from B to U can be detected and measured simultaneously. With even a modest probe current, which decreases the risk of specimen damage, EDX performs excellently in the analysis of very small areas.

FEG-SEM and SEM-EDX analyses were performed on specimens (without preparation) using a JEOL FEG SEM 7600F equipped with an EDX system (Jeol JSM2300 with a resolution < 129 eV) operated at 15 keV with a working distance of 8 mm. The acquisition time for the chemical spectra was 300 s with a probe current of 1 nA.

The quantitative analysis of the atomic elements (SEM-EDX) was performed with the integrated Analysis Station software. A two-step analysis procedure was applied to obtain reliable quantitative results for the elemental profiles over the entire cross sections: (i) subtraction of the bremsstrahlung

using the classical "Top Hat Filter" method and (ii) quantification of the area under each atomic peak determined by the ZAF model [25-26].

Fourier-transform infrared spectroscopy (FTIR)

Fourier Transform Infra-Red Spectroscopy (FTIR) can quantify the absorbance and transmittance of infra-red light, resulting from changes in the dipole moment of molecular bonds, which display vibrational patterns. It is a technique commonly used for characterizing substances, for example, organic materials such as polymers, with wide applicability in many different fields [42-44]. Here, this technique is used to observe how the atoms detected by EDX are organized and to discover whether they are molecular constituents.

Thermo Scientific Nicolet iN10 FTIR was used in the attenuated total reflectance (ATR) mode. Samples were directly deposited on the germanium crystal. Spectra were measured using 64 scans at a resolution of 4 cm^{-1} in the frequency range between 600 and 4000 cm^{-1}. They were analyzed with Thermo Scientific™ OMNIC™ Picta™ Software.

Statistical analysis of results [45]

To be able to analyse the results statistically they must first be converted to effective mass, since EDX values are relative percentages of all detected ions:

$M_i = \frac{x_i d_i}{\sum x_i d_i} m$ with $\sum x_i = 1$

M_i = mass of element i (in µg) // x_i = relative percentage of the element i // d_i = mass density of the element i in g/cm^3 // m = mass of total harvested material (in µg) // $x_1+x_2+x_3+...$ = 100%.

Then, from the previous NTA measurements [2], we computed the global size distribution of the particles; because the EDX calculations are done on the surface of each sample, the size distribution interferes in the analysis of this and a link to the mass of their components is required. The SPAN value is 1 when there are as many percentages of particle sizes above and below the average size (perfect Gaussian curve). It is less than 1 when there is a wider distribution of small particles below the average size than of large particles above. In the opposite case, the SPAN values will be greater than 1. The relative percentage of each element is influenced by this particle size distribution observed in EDX, and the ionic concentration may be adjusted using this SPAN value:

$CS_i = M_i * S$.

CS_i = mass of element i (in µg) multiplied by S (particles size distribution or Span value [2]) = concentration of an element i according to the size of the particles in which it is found.

The NTA SPAN formula (DL90-DL10)/DL50 is an indication of the distance between the 10th and 90th percentile, normalized concerning the midpoint. The DL90, DL10, and DL50 are respectively the 90th percentile, the 10th percentile, and the median of particle sizes.

We used SigmaStat version 4 allowing multiple statistical procedures. A Kruskal-Wallis test is used to determine whether or not there is a statistically significant difference between the medians of three or more independent groups. It is considered to be the non-parametric equivalent of a One-Way ANOVA. If the results of a Kruskal-Wallis test are statistically significant, then it is appropriate to conduct Tukey's Test to determine which specific groups differ. Dunn's Test is a single-step pairwise multiple comparison procedure that can be used to identify means that differ significantly from each other.

Results

Lyophilization

The first results obtained are the quantities of material collected from freeze-drying 100 cc of our solutions (Table 1). These confirmed the NTA results: there is no further decrease in the amount of material from successive dilutions beyond 6CH. However, there is a small loss of material during freeze-drying because we find very small clusters of material stuck to the neck of the small freeze-drying bottles. The pure water from our laboratories in polyethylene bottles does not contain particles in measurable or observable quantity.

Table 1: Quantities of dry matter harvested according to the raw material and the manufacturing process

Name	Dil/Dyn	µg/g	**Name**	Potentization	µg/g	**Name**	Dilution	µg/g	**Name**	Potentization	µg/g
Lactose	Trit 1C	**10000**	Cuprum	Trit 1C	**10000**	Cuprum	Trit 1C	**10000**	Kali-m	1C	**9806**
	Trit 2C	**10000**		Trit 2C	**10000**		Trit 2C	**10000**		2C	**65**
	Trit 3C	**10000**		Trit 3C	**10000**		Trit 3C	**10000**		3C	**44**
	4C	**9723**		4C	**9628**		10^{-8}	**9844**		4C	**51**
	5C	**95**		5C	**142**		10^{-10}	**166**		5C	**60**
	6C/30C	**16.8** (mean)		6C/30C	**38.6** (mean)		$10^{-12}/10^{-60}$	**47.3** (mean)		6C/30C	**45.8** (mean)

Table 1. After freeze-drying, dry matter is observed in all bottles as predicted by the NTA measurements. From 6C onwards the weight of this material is constant even at the highest dilutions. During successive triturations, 99 parts of lactose are used, to which one part of the previous trituration is added, so that the starting weight is the same each time. At the first dilution in water, following trituration, note that when a raw material has been added to the lactose at the beginning, with or without dynamization, more than one hundredth of the weight is retained. This is not the case for pure lactose triturated three times – pure lactose seems to protect the glass from attack by deionized water. This protective effect of lactose persists throughout the following dynamizations/dilutions, so this phenomenon is not related only to the physical presence of lactose. This protective effect apparently does not appear when a raw material has been added to the lactose before the first trituration. The additional weight of material obtained in this case is probably due to a different and specific reaction of the deionized water with the glass since this additional quantity is the same amount as that observed when aaw material is directly dissolved in water (see an example of Kalium muriaticum). From the outset, the triturated raw material plays an obvious role.

SEM

Irrespective of their quality, the SEM images of our samples cannot be analyzed objectively (Figure 1). The only conclusion that can be drawn is that the observed materials have very complex shapes. Three different fields of each sample were photographed (SEM) and measured (EDX). For the analysis, we use the averages of the three observations.

Figure 1: Some illustrative photographs obtained with SEM.

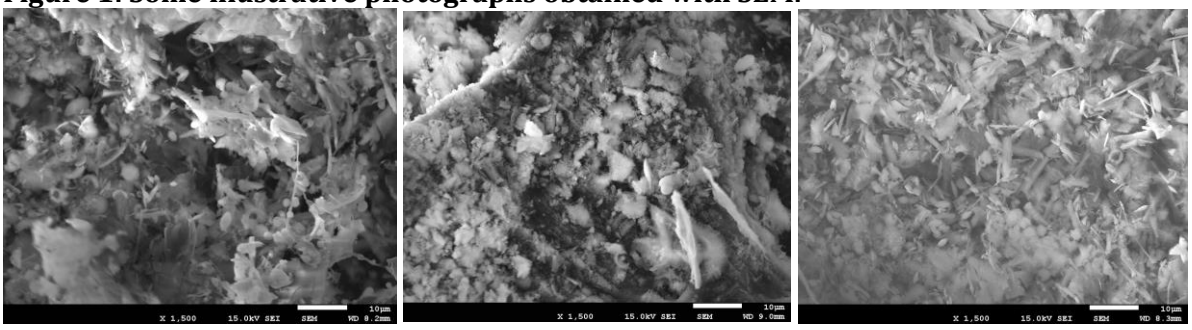

Fig.1 Scale of magnification: 1500 times. On the left Lactose 11C followed by Cuprum 27C and Cuprum 10^{-28} on the right. Differences in structure seem to be present but a mathematical analysis of these images is not possible because of their low resolution, they can only be used as illustrations.

SEM and SPAN (NTA)

Since we note that the results of the NTA measurements are confirmed, it is interesting to compare the data from each. By ranking the SEM-EDX data according to SPAN, which is the range of particle size dispersion in solution normalized by its midpoint, we see that lactose is mainly in the low SPAN value areas and simple dilutions in the higher ones (Table 2).

Table 2: SPAN (S) values versus medicines and dilutions or potentizations.

S	Medicine & Dil/Dyn	S	Medicine & Dil/Dyn	S	Medicine & Dil/Dyn	S	Medicine & Dil/Dyn	S	Medicine & Dil/Dyn
0.75	*Cuprum 10^{-8}*	0.92	Lactose C22	1.02	**Cuprum C14**	1.11	*Cuprum 10^{-24}*	1.26	**Cuprum C18**
0.77	**Cuprum C4**	0.92	Lactose C19	1.03	**Cuprum C6**	1.11	**Cuprum C26**	1.26	*Cuprum 10^{-20}*
0.8	Lactose C10	0.92	Lactose C27	1.03	Lactose C9	1.13	**Cuprum C21**	1.27	*Cuprum 10^{-48}*
0.8	Lactose C25	0.94	Lactose C17	1.03	*Cuprum 10^{-38}*	1.13	Lactose C15	1.28	**Cuprum C15**
0.81	Lactose C4	0.94	**Cuprum C22**	1.04	**Cuprum C30**	1.15	Lactose C18	1.33	**Cuprum C16**
0.82	Lactose C13	0.95	Lactose C26	1.05	**Cuprum C10**	1.15	*Cuprum 10^{-54}*	1.4	*Cuprum 10^{-28}*
0.82	Lactose C24	0.95	Lactose C28	1.05	**Cuprum C24**	1.16	*Cuprum 10^{-16}*	1.43	**Cuprum C20**
0.83	Lactose C14	0.96	Lactose C20	1.06	**Cuprum C25**	1.17	*Cuprum 10^{-14}*	1.46	*Cuprum 10^{-46}*
0.84	Lactose C16	0.96	Lactose C21	1.06	Lactose C7	1.17	**Cuprum C19**	1.46	*Cuprum 10^{-58}*
0.86	Lactose C23	0.96	*Cuprum 10^{-30}*	1.06	*Cuprum 10^{-12}*	1.18	**Cuprum C29**	1.49	*Cuprum 10^{-40}*
0.87	Lactose C29	0.97	*Cuprum 10^{-10}*	1.08	Lactose C5	1.2	**Cuprum C28**	1.66	*Cuprum 10^{-44}*
0.88	Lactose C11	0.99	**Cuprum C8**	1.08	**Cuprum C7**	1.2	**Cuprum C17**	1.74	**Cuprum C12**
0.88	*Cuprum 10^{-22}*	0.99	**Cuprum C5**	1.08	**Cuprum C27**	1.2	*Cuprum 10^{-32}*	1.83	*Cuprum 10^{-56}*
0.9	Lactose C30	1.01	*Cuprum 10^{-18}*	1.09	**Cuprum C13**	1.22	**Cuprum C11**	1.91	*Cuprum 10^{-60}*
0.91	*Cuprum 10^{-26}*	1.02	*Cuprum 10^{-36}*	1.1	Lactose C6	1.25	Lactose C8	1.98	*Cuprum 10^{-52}*
0.92	*Cuprum 10^{-34}*	1.02	**Cuprum C9**	1.1	**Cuprum C23**	1.25	*Cuprum 10^{-50}*	2.92	*Cuprum 10^{-42}*
0.92	Lactose C12								

Table 2. Classification of dilutions or potentizations of manufacturing lines about particle size dispersion in solution normalized by its midpoint. Particle size may influence the structure and composition of harvested material. The first liquid dilutions all have the narrowest particle size distribution but thereafter there is no obvious relation to the degree of dilution. Lactose potentizations are mostly in the small sizes (left), simple dilutions in the wide particle size distribution (right). To facilitate the overview, simple dilutions of copper are in italic, potentized cuprum metalicum are in bold. For the statistical significance of S, values see reference number 2. Highlighted are first soluble dilutions containing almost lactose.

EDX

Three different fields of each sample (lyophilization of a pool of 6 manufacturing lines) are measured by X-ray spectroscopy (Table 3). Each measured atom is quantified relative to the overall percentage of the ions detected. When the percentage is around 0.5, the reliability of the measurement is questionable because the risk of error in this quantification becomes significant. The two most abundant constituents are carbon and oxygen, but these must be interpreted with caution. The sample is placed on a carbon disk, and if it does not cover this completely, the carbon of the support will be measured. The measurements are made under a vacuum, but during handling, ambient oxygen could be incorporated into the sample. Another artefactual source is the contamination of the samples in the SEM analysis chamber by carbon or oxygen.

Table 3: Examples of EDX analysis of the highest dynamizations (30C) of Lactose control and Cuprum metallicum.

Lactose 30CH		Zone 1		Zone 2		Zone 3			
	keV	Atom Percent	Error	Atom Percent	Error	Atom Percent	Error	Mean	Mean error
C_K	0.277	24.43	0.19	23.91	0.20	35.34	0.20	**27.89**	0.20
O_K	0.525	53.94	0.74	55.00	0.80	49.61	0.80	**52.85**	0.78
Na_K	1.041	12.73	0.37	13.85	0.41	10.24	0.40	**12.27**	0.39
Mg_K	1.253	0.99	0.32	1.29	0.35	0.92	0.35	**1.07**	0.34
Al_K	1.486	*0.54*	0.36	*0.16*	0.39	*0.18*	0.39	*0.29*	**0.38**
Si_K	1.739	2.85	0.45	3.34	0.49	1.90	0.49	**2.70**	0.48
S_K	2.307	*0.05*	0.49	*0.05*	0.53	*0.04*	0.53	*0.05*	**0.52**
Cl_K	2.621	*0.15*	0.59	*0.10*	0.64	*0.07*	0.64	*0.11*	**0.62**
K_K	3.312	*1.28*	0.93	*0.58*	1.01	*0.43*	1.01	*0.76*	**0.98**
Ca_K	3.690	2.77	1.15	1.64	1.25	1.21	1.24	**1.87**	1.21
Cu_K	8.040	*0.27*	6.84	*0.09*	7.41	*0.09*	7.38	*0.15*	**7.21**
Tot %		100		100		100		100	
Fit. Breamstrallung		0.6093		0.6069		0.6329			
Fit. ZAF modèle		0.5867		0.5818		0.6070			
Cuprum 30CH		Zone 1		Zone 2		Zone 3			
	keV	Atom Percent	Error	Atom Percent	Error	Atom Percent	Error	Mean	Mean error
C_K	0.277	23.53	0.22	33.62	0.22	29.59	0.23	**28.91**	0.22
O_K	0.525	52.01	0.89	49.17	0.88	50.15	0.92	**50.44**	0.90
Na_K	1.041	15.08	0.45	11.10	0.45	13.68	0.46	**13.29**	0.45
Mg_K	1.253	1.44	0.39	1.03	0.38	1.26	0.40	**1.24**	0.39
Al_K	1.486	*0.37*	0.44	*0.10*	0.44	*0.15*	0.45	*0.21*	**0.44**
Si_K	1.739	3.03	0.54	2.96	0.54	2.51	0.56	**2.83**	0.55
S_K	2.307	*0.18*	0.59	*0.11*	0.59	*0.14*	0.61	*0.14*	**0.60**
Cl_K	2.621	*0.36*	0.71	*0.16*	0.71	*0.24*	0.73	*0.25*	**0.72**
K_K	3.312	*1.13*	1.12	*0.47*	1.11	*0.70*	1.15	*0.77*	**1.13**
Ca_K	3.69	2.68	1.39	1.19	1.38	1.49	1.43	**1.79**	1.40
Cu_K	8.04	*0.20*	8.24	*0.08*	8.18	*0.09*	8.48	*0.12*	**8.30**
		100		100		100		100	
Fit. Breamstrallung		0.6526		0.6567		0.6584			
Fit. ZAF modèle		0.6314		0.6320		0.6350			

Table 3. These two examples of 30CH dynamization do not show a significant difference in the percentages of the different atoms observed on the surface of the particles. The same is not true for lower dilutions. These values are relative and must be corrected by taking into account the amount of material collected and the particle size distribution (SPAN). In EDX, elements are identified by the detection of their electrons, the letter K refers to the n value that electrons in that shell have (K electrons, closest to the nucleus, are n=1 electrons). The calibration of the EDX device to get the best resolution is indicated as fit for "Breamstrallung" or deceleration radiation and fit for "ZAF" or corrections needed when performing semi-quantitative analysis taking into account atomic number (Z) effect, absorption (A) effect, and fluorescence excitation (F) effect.

The amount of collected material and particle size distribution must first be converted to effective mass and correlated with the particle size distribution (SPAN) already obtained from previous NTA measurements (Table 4).

Table 4: EDX mass of elements taking into account the quantities of harvested material and particle size distribution of Cuprum simply diluted, potentized Cuprum, and potentized Lactose.

Cuprum Dil	**10^{-8}**	**10^{-10}**	**10^{-12}**	**10^{-14}**	**10^{-16}**	**10^{-18}**	**10^{-20}**	**10^{-22}**	**10^{-24}**	**10^{-26}**	**10^{-28}**	**10^{-30}**	**10^{-32}**	**10^{-34}**	**10^{-36}**	**10^{-38}**	**10^{-40}**	**10^{-42}**	**10^{-44}**	**10^{-46}**	**10^{-48}**	**10^{-50}**	**10^{-52}**	**10^{-54}**	**10^{-56}**	**10^{-58}**	**10^{-60}**
C	7396,68	159,27	49,94	46,39	53,89	43,18	48,81	28,43	41,31	34,71	49,33	37,52	50,23	39,13	38,07	45,73	63,14	118,25	55,60	59,86	46,82	45,09	71,04	34,52	67,35	40,84	52,40
O	2,08	0,04	0,01	0,03	0,01	0,02	0,04	0,04	0,04	0,03	0,06	0,03	0,03	0,02	0,03	0,02	0,03	0,07	0,07	0,04	0,05	0,05	0,08	0,06	0,06	0,07	0,08
Na	0,47	0,50	0,11	4,41	0,61	2,26	4,29	6,81	6,42	4,15	8,50	4,64	3,67	2,30	5,50	1,77	4,09	11,61	13,44	4,63	7,72	7,95	14,32	8,47	8,86	11,45	15,20
Si	0,38	0,23	0,04	2,08	0,17	1,33	3,89	3,17	2,54	1,99	4,62	1,34	1,57	1,05	2,38	0,67	1,64	2,19	4,28	2,06	2,92	2,64	3,48	7,89	6,70	10,21	14,60
Ca	0,26	0,09	0,02	1,37	0,08	0,62	1,67	1,19	1,07	0,92	1,76	0,77	0,70	0,52	1,08	0,29	0,84	2,96	2,18	1,25	1,23	1,57	1,93	1,77	1,86	4,13	4,65
K	0,28	0,03	0,00	0,17	0,03	0,08	0,15	0,35	0,36	0,23	0,37	0,24	0,16	0,17	0,20	0,06	0,19	0,47	0,64	0,29	0,47	0,39	0,73	0,42	0,45	0,63	0,58
Mg	0,00	0,06	0,01	0,73	0,06	0,36	0,79	1,02	0,96	0,78	1,49	0,93	0,49	0,40	1,00	0,31	0,64	2,76	2,09	0,77	1,04	1,27	2,01	1,36	1,18	1,68	2,99
Cuprum cH	**4C**	**5C**	**6C**	**7C**	**8C**	**9C**	**10C**	**11C**	**12C**	**13C**	**14C**	**15C**	**16C**	**17C**	**18C**	**19C**	**20C**	**21 C**	**22 C**	**23 C**	**24 C**	**25 C**	**26 C**	**27 C**	**28 C**	**29 C**	**30 C**
C	7423,44	140,70	30,19	35,79	31,70	22,81	37,67	31,78	56,14	31,11	26,40	38,22	35,45	37,95	37,16	35,16	46,69	27,13	24,73	38,47	34,34	35,79	31,23	38,99	40,98	33,45	28,69
O	1,86	0,02	0,03	0,02	0,03	0,04	0,02	0,05	0,04	0,03	0,04	0,04	0,05	0,03	0,04	0,03	0,03	0,04	0,03	0,02	0,02	0,02	0,04	0,01	0,02	0,03	0,03
Na	0,30	0,25	5,63	3,30	3,76	9,21	1,51	9,10	5,24	6,28	7,11	6,37	9,56	4,92	5,54	5,82	4,03	8,71	6,44	2,31	2,21	2,81	5,74	1,45	2,70	5,92	5,81
Si	2,55	0,11	1,51	1,17	1,31	3,41	0,61	2,70	3,42	1,37	2,20	2,09	2,71	1,70	3,57	1,87	2,76	3,45	2,34	0,66	2,52	1,28	3,12	0,80	1,34	3,29	2,98
Ca	0,25	0,05	1,31	0,81	0,82	1,95	0,36	1,63	1,29	1,52	2,17	1,34	1,80	0,95	1,17	1,04	0,95	2,23	1,49	0,42	0,94	0,61	1,41	0,27	0,62	1,44	1,29
K	0,00	0,01	0,28	0,16	0,23	0,48	0,07	0,56	0,22	0,36	0,44	0,30	0,55	0,21	0,19	0,26	0,16	0,47	0,29	0,11	0,10	0,12	0,32	0,06	0,13	0,28	0,30
Mg	0,00	0,03	0,83	0,38	0,50	1,50	0,19	1,26	0,81	1,50	1,13	0,90	1,27	0,60	0,82	0,79	0,52	1,75	0,96	0,36	0,36	0,39	0,93	0,21	0,39	0,95	0,97
Lactose cH	**4C**	**5C**	**6C**	**7C**	**8C**	**9C**	**10C**	**11C**	**12C**	**13C**	**14C**	**15C**	**16C**	**17C**	**18C**	**19C**	**20C**	**21 C**	**22 C**	**23 C**	**24 C**	**25 C**	**26 C**	**27 C**	**28 C**	**29 C**	**30 C**
C	7914,92	102,18	15,15	11,86	18,76	16,65	12,51	9,67	15,15	13,28	13,69	18,05	13,99	14,66	18,42	15,32	15,48	15,79	14,18	12,70	10,64	10,55	10,37	12,32	13,66	8,97	10,92
O	2,33	0,04	0,01	0,02	0,01	0,00	0,01	0,01	0,00	0,00	0,00	0,01	0,00	0,01	0,01	0,00	0,00	0,00	0,01	0,01	0,01	0,01	0,01	0,01	0,01	0,01	0,01
Na	0,68	0,45	1,67	3,00	1,22	0,36	0,48	2,44	0,12	0,29	0,15	0,43	0,08	0,71	0,54	0,05	0,35	0,15	0,69	1,01	1,62	1,69	3,05	1,78	1,13	2,78	2,12
Si	0,00	0,17	0,93	1,58	0,59	0,20	0,23	1,20	0,03	0,06	0,12	0,28	0,01	0,11	0,10	0,03	0,10	0,10	0,26	0,34	0,70	0,63	1,21	0,67	0,71	1,47	1,12
Ca	0,00	0,07	0,39	0,67	0,22	0,07	0,10	0,62	0,03	0,03	0,01	0,10	0,01	0,08	0,10	0,02	0,05	0,05	0,11	0,18	0,47	0,27	0,62	0,33	0,21	0,74	0,53
K	0,00	0,03	0,05	0,12	0,05	0,01	0,02	0,14	0,01	0,01	0,00	0,02	0,00	0,04	0,04	0,00	0,02	0,01	0,04	0,03	0,07	0,08	0,14	0,09	0,04	0,14	0,12
Mg	0,00	0,04	0,20	0,48	0,11	0,06	0,08	0,62	0,02	0,05	0,01	0,09	0,01	0,12	0,09	0,01	0,04	0,02	0,09	0,11	0,24	0,23	0,48	0,25	0,15	0,43	0,33

Table 4. Mass of element in µg*SPAN of potentization. Products previously triturated in lactose have a higher carbon and oxygen composition (the main components of lactose) at the outset. The amounts of sodium are significantly lower in the potentized lactose compared to production lines where raw material was incorporated at the beginning. Copper is not a significant component, being present only at the beginning of the manufacturing process and absent in later dilutions.

OPEN ACCESS

FTIR

We can see that in all these production lines the main component is sodium hydrogen carbonate (Figure 2), thus confirming that the common presence of carbon, oxygen, and sodium found by EDX is not due to measurement bias.

Figure 2: Example of an FTIR profile.

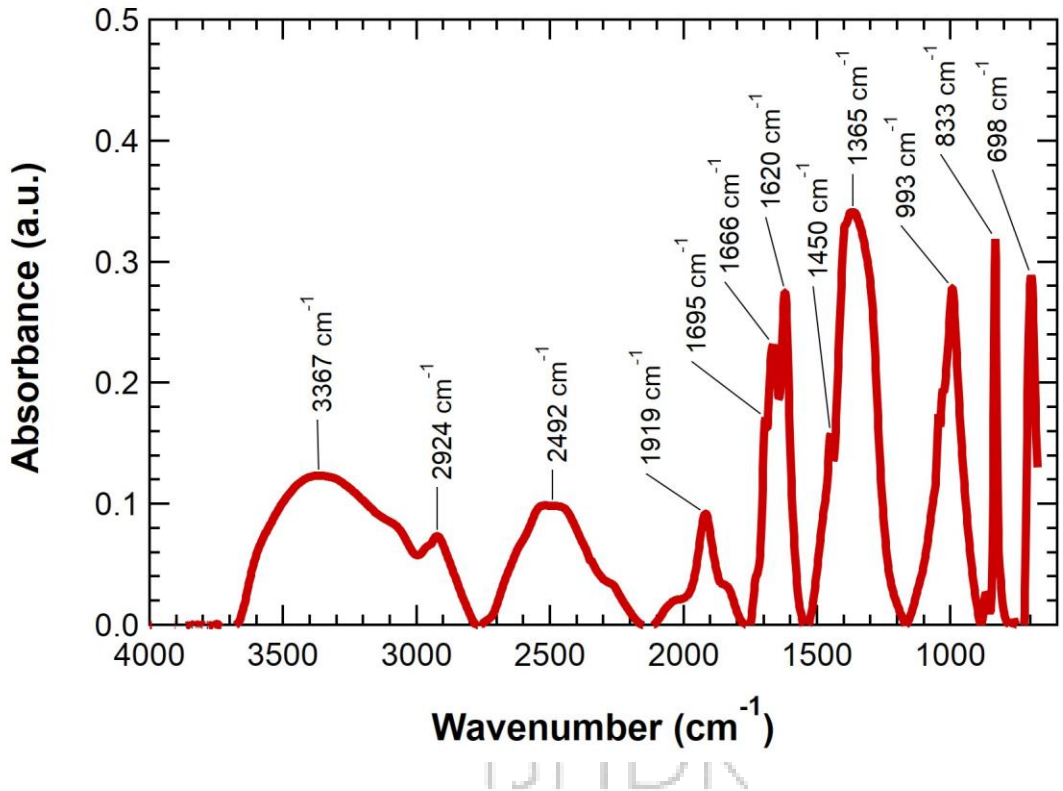

Fig.2 The measured spectrum is characteristic of sodium bicarbonate [44] except for the broad peak around 3367 cm^{-1} due to adsorbed water. The peaks at 2924 and 2492 cm^{-1} may be attributed to O-H moieties, those at 1695, 1666, and 1620 cm^{-1} to C=O moieties, and that at 1365 cm^{-1} to C-OH moieties. Sodium hydrogen carbonate is the monosodium salt of carbonic acid with alkalinizing and electrolyte replacement properties. Upon dissociation, sodium hydrogen carbonate forms sodium and bicarbonate ions. Both ions decrease hydrogen ion concentration, resulting in raised pH. This compound is systematically identified in all these manufacturing lines. Systematic analyses of the variations of these profiles from one raw material to another are in progress.

Statistical results (Table 5):

Table 5: Statistical comparison of potentized cuprum metallicum, potentized lactose, and simply diluted copper for the significant elements: carbon, oxygen, sodium, silicon, calcium, and magnesium.

Stats	"C" Diff of Ranks	"C" Q values	**"C" p values**	"O" Diff of Ranks	"O" Q values	**"O" p values**	"Na" Diff of Ranks	"Na" Q values	**"Na" p values**	"Si" Diff of Ranks	"Si" Q values	**"Si" p values**	"Ca" Diff of Ranks	"Ca" Q values	**"Ca" p values**	"Mg" Diff of Ranks	"Mg" Q values	**"Mg" p values**
W* Lact cH/Cu cH	26.333	4.113	**<0.001**	30.667	4.789	**<0.001**	30.407	4.749	**<0.001**	33.444	5.223	**<0.001**	32.630	5.096	**<0.001**	28.815	4.500	**<0.001**
W* Cu cH/Cu Dil	16.889	2.638	**0.025**	6.778	1.059	0.869	2.296	0.359	1	1.556	0.243	1	0.296	0.0463	1	3.593	0.561	1
W* Lact cH/Cu Dil	43.222	6.750	**<0.001**	37.444	5.848	**<0.001**	32.704	5.107	**<0.001**	33.444	5.223	**<0.001**	32.926	5.142	**<0.001**	32.407	5.061	**<0.001**
L* Lact cH/Cu cH/Cu Dil			** 0.058			** 0.216			** 0.386			** 0.203			** 0.148			** 0.441
H* Lact cH/Cu cH	21.737	4.036	**<0.001**	24.632	4.574	**<0.001**	23.895	4.437	**<0.001**	24.842	4.613	**<0.001**	25.211	4.681	**<0.001**	23.842	4.427	**<0.001**
H* Cu cH/Cu Dil	13.526	2.512	**0.036**	7.421	1.378	0.505	6.211	1.153	0.746	3.842	0.713	1	3.263	0.606	1	7.263	1.349	0.532
H* Lact cH/Cu Dil	35.263	6.548	**<0.001**	32.053	5.952	**<0.001**	30.105	5.590	**<0.001**	28.684	5.327	**<0.001**	28.474	5.287	**<0.001**	31.105	5.776	**<0.001**

* **W** = whole manufacturing lines 4cH up to 30cH or equivalent simple dilutions. **L** = low potentizations or equivalent dilutions 4cH up to 11cH. **H** = High potentizations or equivalent dilutions 12cH up to 30cH.
** The differences in the median values among the treatment groups are not great enough to exclude the possibility that the difference is due to random sampling variability; there is no statistically significant difference.

Table 5. In pairwise multiple comparison procedures (Dunn's test) Difference of Ranks between different identified elements (C, O,Na, Si,Ca, Mg) in 2 or more manufacturing lines is calculated determining the statistical Q values and the p statistical validity of these values. The above statistical comparisons of Potentized Cuprum metallicum and Potentized Lactose confirm differences for all elements in the full manufacturing lines (4cH to 30cH); within these, it is the high potentizations (12cH to 30cH) that show significant differences whilst the lower potentizations (4cH to 11cH) do not. These differences exist whether potentized lactose is compared with copper either potentized or simply diluted. Potentized Cuprum metallicum and simply diluted copper differ only for the element carbon, but this result must be interpreted with caution because the sample is analyzed on a carbon support.

OPEN ACCESS

Discussion

Visually, we can see differences between crystal forms in the SEM images, but these cannot be formally objectified due to the low quality of the pictures. Neither can the relative atomic percentages measured by EDX lead us to a clear conclusion.

The large quantities of the three main elements (carbon, oxygen, and sodium) are obvious. However, the carbon content may depend on the amount of material available, the uniformity of its application to the carbon support, and contamination by the carbon which is always present in the analysis chamber. Oxygen can vary with time; the powder is exposed to air during handling. We can reduce the risk of errors by taking three measurements from different areas of the same sample. It is necessary to convert these relative percentages into mass, which we can do since we know the weight of each sample collected by freeze-drying. Moreover, because EDX measures surface atoms, the quantities will depend on the exposed surface area and therefore on the sizes of the particles that comprise this. Because we already know the size distribution of these from our previous NTA (SPAN) measurements [2], it is valid to use this additional parameter in the statistical analysis of the results.

Since the atoms detected derive mainly from sodium bicarbonate, we may question its source since this molecule does not exist in the raw materials. Carbon and oxygen are components of lactose used for the trituration of insoluble materials, which might explain their presence. But they are also found in soluble materials, in which case they might come from the ambient air (CO_2) during the manufacturing process.

The sodium, with its constant presence throughout the dilutions, can only come from the pharmaceutical glass used. This soda-lime glass, with a coefficient of expansion of 7.8 (amber – PhEUR - Type 3), consists of 67% of SiO_2, 12% of Na_2O, 7% of Al_20_3, 5% of Mg, 2% of Fe_20_3, 1% of CaO, 1% of K_2O and less than 0.5% of MnO_2. Silicates are very hard and will not come off the glass easily, whilst alternatively, soft salts such as Na_2O can easily be released from the glass. The solvent used (pure water) is active upon glass and strongly attracts ions; this may explain the stability of concentrations of sodium beyond a certain dilution level. It also explains the presence of traces of aluminum, magnesium, iron, and calcium.

One could argue that water contains always bicarbonate ions, and that pure water does not exist. Indeed, in surface water the carbonate cycle is well known to everyone: $CO_2 + H_2O = H_2CO_3$ (Carbonic acid); $H_2CO_3 + H^+$ produce bicarbonate; $CO_3^{2-} + H^+$ produce carbonate. These carbonates can bind to magnesium, calcium, potassium, or sodium depending on the pH and hardness (total concentration of calcium and magnesium ions) of the water. This natural phenomenon does not explain the abnormally high level of sodium hydrogen carbonate.

How is it possible that the compositions can vary due to the presence of a single raw material? We have seen that the main component of these solutions is sodium hydrogen carbonate. It is known that when the free CO_2 content of the water remains constant, active CO_2 will be transformed into equilibrating CO_2, with the formation of $NaHCO_3$ [46]. The structure of this molecule is well known [47]; it interacts strongly with the water molecules surrounding it. This phenomenon is dynamic and is also influenced by temperature. Its pH is high which generates local electric fields in the solutions. As the quantities of this molecule and other salts, mainly silica, calcium, and magnesium, may vary depending on the raw material used at the beginning, we may hypothesize that a unique composition is possible depending on the electric field generated and also on the dynamization process. This hypothesis must be verified by pH measurement. We already know that the orientation of the molecular dipoles is remedy-specific [5-8].

OPEN ACCESS

Following the European Pharmacopoeia [23], first dilutions of a soluble MT (Mother Tincture) must be prepared using the same alcohol concentration as the MT to avoid precipitates, but alcohol is not required for higher dilutions when producing homeopathic medicines. When a homeopathic medicine is made for bulk storage in a pharmacy, 62% w/w alcohol is added as a preservative, but intermediate dilutions are always prepared in pure water and then discarded. All Korsakov intermediate preparations are similarly prepared using pure water (Hahnemann approved this process in a letter to Korsakov), and alcohol is added only for the final dynamizations. It is assumed that the homeopathic information is carried by the water solvent and not by the alcohol. The NTA measuring cell would be damaged by solutions containing alcohol, and the lyophilization process is adapted for aqueous solutions.

The idea that homeopathic medicines are non-material, propounded by both opponents of homeopathy and by traditional homeopathic practitioners, cannot be maintained given these findings. Science is based upon measurement; measurements are facts that cannot be disputed. Nevertheless, the presence of these particles does not allow us to conclude that the effect of homeopathy is due only to a classical molecule-receptor interaction. Given that the final product (impregnated pills, globules, granules, etc.) contains only a very small quantity of the medicine in question, a different pathway is much more likely. To verify this assertion, other methodologies, such as Nuclear Magnetic Resonance, pH, infrared measurements, and/or Electro-photonic analysis are needed.

It is important to recognize that there is a large difference between the quantities of material obtained from different stocks. The hypothesis of nanobubble formation during the trituration process is plausible for insoluble materials such as metals (e.g. copper), although this hypothesis has yet to be verified. During the lyophilization process, all gas bubbles are eliminated and only the dry matter is examined, so the role of nanobubbles cannot be studied by this technique.
Throughout these measurements, all manufacturing variables were tightly controlled: same environment, same water, same glass, same machines, same stock, and same staff for each step of fabrication and measurement. While these controls strengthen the results, one must be careful with any generalization from these conclusions, because so many different homeopathic medicines exist and in different concentrations. In the future, it will be possible to study the impact of certain changes in parameters such as the use of different types of glass containers, the number of dynamizations, etc.
All measurements were carried out using samples prepared without alcohol, and previous measurements of NMR relaxation times also required preparations made with pure water. However, for pH measurements and electro-photonic analysis, it will be possible to use commercial homeopathic medicines kept in a mixture of water and alcohol.

SEM-EDX alone does not permit significant discrimination between single C potentization at different levels; only the combination of results allows complete manufacturing lines to be discriminated against. The great variability in the size of particles is an indication of the very complex shapes of particles in homeopathic medicines, and this complexity must be taken into account when studying any mechanism of action of these medicines.

The role of sodium hydrogen carbonate seems essential given the dominant concentration of sodium. Nevertheless, this role may be modulated by the variable quantities observed, the size of these molecules interacting with the environment, and the presence of other smaller components, formed mainly by silica, calcium, or magnesium.

OPEN ACCESS

Dynamization versus dilution

Whilst the dilution factor is part of the potentization process, it is the dynamization itself that produces detectable changes in the particles' structure [2], but not in the partition of ions. It is important to emphasize the fact that we recovered quite stable concentrations of material in all diluted/dynamized manufacturing lines, but when the dynamization process is not applied (simple dilution process), the ion partition becomes unstable. The dynamization process does not affect the amount of material present but instead creates specific shapes and compositions; these important differences justify further studies of the behavior of the solvent surrounding these specific particles. Simple dilution was begun after three triturations in lactose (1C, 2C, 3C), from which point the simple dilution process was done step by step without shaking. We observed then that the ion partitions were much more heterogeneous than when the process included dynamization. Variations in the number of particles at each step likely may to some extent buffer the deionized water differently concerning its ability to attack the pharmaceutical glass. During the simple dilution process, this effect would become more and more noticeable, causing larger and larger variabilities in particle size distribution. Dynamisation homogenizes each preparation step, allowing the particle size distributions to become increasingly stable. These results need to be confirmed on other manufacturing lines and other raw materials – for example, a soluble potentized raw material shows more variability in the ion partition.

Limitations of the current study

This study was carried out according to Good Pharmaceutical Practice (GPP). It would be helpful to compare these results concerning Good Manufacturing Practice (GMP) and to compare them with results obtained using other batches and other stocks. Reproducibility by other laboratories using the same framework also needs to be demonstrated. Each measurement and sample preparation technique has its limitations and interactions with the product. The process of freeze-drying loses not only any gaseous particles but also the very light components. We have observed that tiny particles stick to the small balloon connection reducer used in the second phase of lyophilization, and analysis of these showed that they are composed of the same atoms as those of the preserved material. This does not change the validity of our measurements qualitatively, but the lightest particles are lost during this process. Whilst the effect of this loss will be similar for all samples, we cannot exclude the possibility that some raw materials will produce more light particles than others, resulting in a larger loss of material. Measurements were carried out on preparations without alcohol to ensure accurate results. Other techniques are required for which alcohol does not compromise the accuracy of the measurement so that a comprehensive picture of the nature of homeopathic medicines can be developed. Even though our measurements identified differences between homeopathic medicines and controls, many questions remain, such as the specificity of the signature between different homeopathic stocks of the same family (plant/metal/others), or between each dynamization level, which cannot be addressed by this single study.

Implications for future research

To address the problem of plausibility [18] of homeopathic medicines, more pharmacological studies are needed. The present measurements justify further research and demonstrate the importance of GPP and excellent quality control for the MT. It also opens new perspectives for further research areas and alternative explanations of the mechanism of action of homeopathic medicines. Research on homeopathic medicines must not remain anecdotal but should be integrated into the pharmaceutical training of future pharmacists. This research project must continue and carry out more systematic particle measurements, as has already taken place [1-2] using other approaches such as NMR measurements [13-14] as well as infrared spectroscopy and electric field measurements.

Conclusions

Using a step-by-step dilution or potentization process, SEM-EDX findings revealed the presence of dry matter with a crystalline structure and ions in all samples (except for pure water in PET containers), even at the highest level of dilution. By converting the relative percentages of atoms by mass and taking into account the varieties of forms, it becomes possible to discriminate the raw materials from each other.

We can confirm that potentized medicines made in glass containers do contain dry material which can only be explained by a reaction between the deionized water and the glass because the composition was consistent at each step of the potentization process. The molecular formation and partition of ions indicate a broadly diverse but specific phenomenon; the initially concentrated raw material drives this partition when the process includes dynamization.
We conclude that at each step of manufacturing a homeopathic medicine, a different but coherent and specific ion, and molecular partition is generated, initiated by the specific starting material, which will react with the solvent and glass container uniquely. Further measurements are needed to support these findings, using other raw materials with the same controls (solvent and simply diluted manufacturing lines).

The ion partition depends upon the source material but not the potentization. The images of simply diluted compounds lose homogeneity.
Further investigations are needed to confirm that the essential component of these homeopathic medicines is sodium hydrogen carbonate, modulated by some other elements and by its quantity, size, and shape.

Acknowledgment

Private donations from patients and MDs and support from UNIO HOMOEOPATHICA BELGICA (Belgian MD Homeopathic Union) financed this study. The necessary copper stock was provided by the REMEDY BANK® cooperative company. PHARAHOM (Belgian homeopathic pharmacists' association) financed the manufacturing process. Part of the SEM-EDX and FTIR experiments were performed by Clara Coussement. We thank them all.
The authors also wish to acknowledge the kind assistance of Galen Ives in correcting the final proofs.

Disclosure

No conflict of interest exists. This study has been funded by private donations.

References

[1] Van Wassenhoven M, Goyens M, Capieaux E, Devos P, Dorfman P. (2018). Nanoparticle Characterisation of Traditional Homeopathically Manufactured Cuprum metallicum and Gelsemium sempervirens Medicines and Controls. Homeopathy: 2018 Nov;107(4):244-263.
[2] Van Wassenhoven M, Goyens M, Dorfman P, Devos P. (2021). Particle Characterisation of Traditional Homeopathically Manufactures Medicine Cuprum metallicum and Controls. Int J High Dilution Res. 2021; 20 (4): 11-28.
[3] Konovalov AI, Ryzhkina IS, Murtazina LI, Kiseleva LV (2014). Forming the nanosized molecular assemblies (nonoassociates) is a key to understand the properties of highly diluted aqueous solutions. Biofizica May-Jun 2014;59(3)421-7.
[4] Ives JA, Moffett JR, Arun P, Lam D, Todorov TI, et al. (2010). Enzyme stabilisation by glass-derived silicates in glass-exposed aqueous solutions. Homeopathy 99:15-24.
[5] Cartwright S (2014). Pyridinium-N-phenolates as molecular probes of serially diluted and agitated solutions: preliminary results. Homeopathy 103:65.
[6] Cartwright SJ. Solvatochromic dyes detect the presence of homeopathic potencies. Homeopathy (2015), http://dx.doi.org/ 10.1016/j.homp.2015.08.002. 1-11
[7] Cartwright SJ. (2017). Interaction of homeopathic potencies with the water soluble solvatochromic dye bis-dimethylaminofuchsone. Part 1: PH studies. Homeopathy (2017) 106, 37-46
[8] Aparicio AC, de Oliveira LH, Silva JS, Coelho CP, Pinheiro SR, Souza MF, Suffredini IB, Cartwright S, Bonamin LV. (2014). Experimental evidence of stable water nanostructures in extremely dilute solutions, at standard pressure and temperature. Homeopathy (2014) 103, 44-50
[9] Elia V, Ausanio G, Gentile F, Germano R, Napoli E, and Niccoli M. (2013). Experimental Evidence of Stable Aggregates of Water at Room Temperature and Normal Pressure After Iterative Contact with a Nafion® Polymer Membrane. Water (Australia) 2013;5:16-26.
[10] Demangeat JL (2015). Gas nanobubbles and aqueous nanostructures: the crucial role of dynamisation. Homeopathy Apr;104(2):101-15
[11] Demangeat JL (2009). NMR water proton relaxation in unheated and heated ultrahigh aqueous dilutions of histamine: Evidence for an air-dependent supramolecular organisation of water. Journal of Molecular Liquids 144;32-39
[12] Demangeat JL (2013). Nanosized solvent superstructures in ultramolecular aqueous dilutions: twenty years' research using water proton relaxation. Homeopathy 2013;102:87-105.
[13] Van Wassenhoven M, Henry M, Goyens M, Capieaux E, Devos P. (2017). Nuclear Magnetic Resonance Characterisation of Traditional Homeopathically-Manufactured Copper (Cuprum metallicum) and a plant (Gelsemium sempervirens) Medicines and Controls. Homeopathy (2017) 106, 223e239
[14] Van Wassenhoven M, Henry M, Goyens M, Cumps J, Devos P. (2021). Verification of Nuclear Magnetic Resonance Characterisation of Traditional Homeopathically

Manufactured Metal (Cuprum metallicum) and Plant (Gelsemium sempervirens) Medicines and Controls. Homeopathy 2021;110:42–51.
[15] Mathie RT, Van Wassenhoven M, Jacobs J & al. (2015). Meta-analysis of randomised, placebo-controlled, trials of individualised homeopathic treatment. European Journal of Integrative Medicine 7:16 DOI: 10.1016/j.eujim2015.09.042
[16] Mathie RT, Roniger H, Van Wassenhoven M, & al. (2012). Method for appraising model validity of randomised controlled trials of homeopathic treatment: multi-rater concordance study. BMC Medical Research Methodology 12:49.
[17] Editorial (2005). The end of homeopathy. Lancet 366:690.
[18] Rutten L, Mathie RT, Fisher P, Goossens M, Van Wassenhoven M. (2013). Plausibility and Evidence: the case of Homeopathy. Medicine, Health Care and Philosophy 16:3/525-532.
[19] Klein S, Würtenberger S, Wolf U, Baumgartner S and Tournier A. (2018). Physicochemical Investigations of Homeopathic Preparations: A Systematic Review and Bibliometric Analysis—Part 1. JACM Volume 24, Number 5, 2018, pp. 409–421
[20] Klein S, Würtenberger S, Wolf U, Baumgartner S and Tournier A. (2018). Physicochemical Investigations of Homeopathic Preparations: A Systematic Review and Bibliometric Analysis—Part 2. JACM Volume 25, Number 9, 2019, pp. 890–901
[21] Klein S, Würtenberger S, Wolf U, Baumgartner S and Tournier A. (2018). Physicochemical Investigations of Homeopathic Preparations: A Systematic Review and Bibliometric Analysis—Part 3. JACM Volume 27, Number 1, 2021, pp. 45–57
[22] Dei A. (2020). Experimental Evidence Supports New Perspectives in Homeopathy. Homeopathy 2020;109:256–260.
[23] European Pharmacopoeia 10.6 (2021)
[24] Mutalib M.Abd, Rahman M.A., Othman M.H.D., Ismail A.F., Jaafar J. (2017). Scanning Electron Microscopy (SEM) and Energy-Dispersive X-Ray (EDX) Spectroscopy. Elsevier. Membrane Characterization. 2017, Chapter 9: Pages 161-179. https://doi.org/10.1016/B978-0-444-63776-5.00009-7
[25] P. Van Espen, R. Van Grieken, A. Markowicz et M. Dekker, In Handbook of X-Ray Spectrometry, Methods and Techniques, New York, 1993, p. 181–293.
[26] J. Osán, J. De Hoog, P. Van Espen, I. Szalóki, C.-U. Ro et R. Van Grieken, X-Ray Spectrometry, Volume 30. Issue 6, 2001, pp. 419-426.
[27] Tsukihara T, Aoyama H, Yamashita E & al (August 1995). "Structures of metal sites of oxidized bovine heart cytochrome c oxidase at 2.8 A". *Science* 269 (5227): 1069–74
[28] Hodiamont. (1970) Homéopathie et Physiologie. Ed Similia ISBN 2-7008-0176-8.
[29] Hahnemann S(1828). Chronic Diseases. Schmidt & Kunzli Ed. Maisonneuve 1969.
[30] Allen T (1879). Encyclopedia of Pure Materia Medica. New York, USA. Boericke & Tafel, Philadelphia, USA.
[31] Bradford T (2000). Index of Homeopathic Provings, New Delhi, India, B Jain Publishers.
[32] Duke J, Hughes R (1891). Cyclopaedia of Drug Pathogenesy, London, UK, Gould; New Delhi, India, B Jain Publishers.

[33] Allen HC (2000). Allens Keynotes. B Jain Publishers, New Delhi, India.
[34] Dorfman P, Guillemain J, Nevy P, Tetau M (1987). Double-Blind Drug pathogenesy of Cuprum metallicum 30CH. Cahiers de Biothérapie 93:47-56.
[35] Mahata CR (2013). Dielectric dispersion studies of some potentised homeopathic medicines reveal structured vehicle. Homeopathy, Vol 102(4):262-267.
[36] Betello CF (2002). Antioxidante effect in vitro of the homeopathic medicine Arsenicum album, Cuprum metallicum, Manganum and Zincum metallicum. Thesis Faculdade de Ciências da Saude de Säo Paulo, Brazil.
[37] Smits T (2013). Inspiring Homeopathy: Treatment of Universal Layers. ISBN 9789076189000.
[38] Van Wassenhoven M (2008). First line medicine – Clinical Verification – Verification of homeopathic symptoms. Cuprum metallicum. ISBN 978-2-87491-003-6. p:212-3/578-9.
[39] Boericke W, Boericke OE (1927). Homeopathic Materia Medica. ISBN 0766183882
[40] Santini R, Tessier M, Bellon P (1991). First experimental arguments in favour of the effect of very weak doses of copper on digestive motricity in mice and rabbits. In:Taylor&Francis. Ultra low doses 3-10.
[41] Hariveau E, Nolen P, Holtzscherer A (1991). A study of the effectiveness of ultra low doses of copper in the treatment of hemodialysis-related muscle cramps. RCT. In: Doutremepuich C (ed) Ultra Low Doses, Taylor&Francis, London, UK 145-149
[42] Khan AS, Khalid H, Sarfraz Z, Khan M, Iqbal J, Muhammad N, et al. Vibrational spectroscopy of selective dental restorative materials. Appl Spectrosc Rev. 2017; 52: 507–540.
[43] Chalmers JM, Everall NJ. FTIR, FT-Raman and chemometrics: Applications to the analysis and characterisation of polymers. TrAC—Trends Anal Chem. 1996; 15: 18–25.
[44] Stein S.E., "Evaluated Infrared Reference Spectra" in NIST Chemistry WebBook, NIST Reference Database 69, Eds. Linstrom P.J. and Mallard W.G., National Institute of Standards and Technology, Gaithersburg MD, 20899 (doi: 10.18434/T4D303)
[45] Peck R, Olsen C and Devore JL. (2008). Introduction to Statistics and Data Analysis (3d ed.). Cengage Learning.
[46] Thieme C; Sodium Carbonates. Ullmann's Encyclopedia of Industrial Chemistry. 7th ed. (1999-2017). New York, NY: John Wiley & Sons. Online Posting Date: 15 Jun 2000.
[47] Taga T. (1969) Crystal structure of $Na_2CO_3.10H_2O$. Acta Crystallographica. Dec. 1969 Vol 25 Issue 12, p.2656-58.

© International Journal of High Dilution Research.
Not for commercial purposes.